Selective modulation of α5 GABAA receptors exacerbates aberrant inhibition at key hippocampal neuronal circuits in APP mouse model of Alzheimer's disease

Alexandra Petrache[1], Archie Khan[1], Martin Nicholson[1], Alessandra Monaco[1], Martyna Kuta-Siejkowska [1], Shozeb Haider[1], Stephen Hilton[1], Jasmina Jovanovic[1], and Afia Ali[1]

[1]University College London School of Pharmacy

May 27, 2020

Abstract

Background and Purpose: Selective negative allosteric modulators (NAMs), targeting α5 subunit-containing GABAA receptors (GABAARs) as potential therapeutic targets for disorders associated with cognitive deficits, including Alzheimer's disease (AD), continually fail clinical trials. We investigated whether this was due to the alteration of synaptic mechanisms associated with α5 GABAARs in AD. Experimental approach: Using medicinal chemistry and computational modelling, we developed aqueous soluble hybrids of 6,6-dimethyl-3-(2-hydroxyethyl)thio-1-(thiazol-2-yl)-6,7-dihydro-2-benzothiophen-4(5H)-one, that demonstrated selective binding and high negative allosteric modulation, specifically for the α5 GABAAR subtype in constructed HEK293 stable cell-lines. Using a knock-in mouse model of AD (APPNL-F/NL-F), which expresses a mutant form of human amyloid-β (Aβ), we performed immunofluorescence studies combined with electrophysiological whole-cell recordings to investigate the effects of our key molecule, α5-SOP002 in the hippocampal CA1 region. Key Results: In aged APPNL-F/NL-F mice, a selective preservation of α5 GABAARs was observed in: dis-inhibitory, calretinin- (CR), cholecystokinin- (CCK), somatostatin- (SST) expressing interneurons, and pyramidal cells. Synaptic inhibition recorded from CR interneurons in APPNL-F/NL-F mice, was abnormally excessive, but was "normalised" with bath-applied α5-SOP002 (1 μM). However, α5-SOP002, further impaired inhibition onto CCK and pyramidal cells that were already largely compromised by exhibiting a deficit of inhibition in the AD model. Conclusions and Implications: Using a multi-disciplinary approach, we show that exposure to α5 GABAAR NAMs may further compromise aberrant synapses in AD. We therefore suggest that the α5 GABAAR is not a suitable therapeutic target for the treatment of AD or other cognitive deficits due to the widespread neuronal-networks that use α5 GABAARs.

Introduction

Over the last few decades, considerable focus has been on negative allosteric modulators (NAMs) (previously referred to as inverse agonists) of the benzodiazepine site of γ -aminobutyric acid receptors ($GABA_A$Rs) as a potential therapeutic target for cognitive impairment in temporal lobe epilepsy (TLE), Huntington's disease, Down's syndrome, schizophrenia and the most common form of dementia, Alzheimer's disease (AD), which constitutes one of the most significant health problems confronting societies with an aging population.

The ionotropic $GABA_A$ R family are heteropentameric structures consisting of a combination of five subunits (Sieghart et al., 2002) with the α-subunit being clinically relevant, as it controls the pharmacological profile of $GABA_A$ Rs (McKernan et al., 1996). Since the understanding that distinct pharmacological properties of the $GABA_A$R are reliant on the fact that different brain regions and cell types contain various subunit compositions, NAMs of the $GABA_A$R at the subunit level have been widely studied. In particular, $GABA_A$Rs containing the *α5-subunit* have been of interest, given their role in learning and memory as evidenced by various studies (Caraiscos et al., 2004; Collinson et al., 2002; Crestani et al., 2002; Dawson et al., 2006; Ghafari et al., 2017; Yee et al., 2004).

The hippocampus plays a critical role in memory formation and retrieval, and is significantly affected in AD, which is characterised by short-term memory deficits as one of the first symptoms of the disease (Price et al., 2001). The strong evidence to suggest hippocampal preferential distribution of the α5-containing $GABA_AR$ sub-type (Quirk et al., 1996), together with its diverse pathology in memory deficit-related disease, and particularly, its preservation in human brains of AD patients (Howell et al., 2000; Rissman et al., 2007), has led many researchers to test several α5 subunit-selective compounds for their potential cognition-enhancing effects (Liu et al., 1996; Quirk et al., 1996; Savic et al., 2008; Sternfeld et al., 2004).

Originally, Merck, Sharp and Dohme, (MSD) developed the first $GABA_AR$ NAM, known as α5IA, with high efficacy at the $GABA_A$ α5 receptor sub-type without being an anxiogenic agent (Atack et al., 2006). Following the development of this compound by MSD, a number of other nootropic drugs (α5 sub-type selective NAMs) have been developed (*e.g.* RO4938581; (Ballard et al., 2009)). Many of these studies reported an impressive pharmacological profile of this compounds and their potential as cognitive enhancers without CNS-mediated adverse effects (Ballard et al., 2009; Braudeau et al., 2011; Chambers et al., 2003; Collinson et al., 2006; Dawson et al., 2006; Duchon et al., 2019; Eimerbrink et al., 2019; Martinez-Cue et al., 2014). These studies were initially implemented in rodent models, and unfortunately, these results were not reproducible in human subjects/patients to the same extent. Several key molecules consistently failed clinical trials at different phases including Basmisanil (code, RO5186582, Roche, 2019), a5IA (Atack, 2010) and MRK-016 (Atack et al., 2009). Basmisanil was taken through Phase 1 and Phase 2 of clinical trials for Down's syndrome and although in the Phase 2, it was shown not to be efficacious in either adults or adolescents. It appears that despite a5IA and MRK-016 demonstrating tolerance in young males, some of these molecules were poorly tolerated in elderly patients with no cognitive improvement (Atack, 2010), thus reducing the viability of α5 as a therapeutic target. Although these molecules were shown to be selective for α5 subunit- containing $GABA_ARs$, the lack of efficacy and poor tolerance in human patients could be related to poor brain penetration of the molecules or an age-related effect.

Whether this failure was due to low drug potency / bioavailability or due to a general lack of understanding of the synaptic mechanisms involving α5 receptors during the pathogenesis of the disease is currently unclear. To address these issues, we synthesised a novel water soluble α5 $GABA_AR$ selective NAM. These receptor sub-types have been shown to be located in hippocampal extrasynaptic sites, as well as synaptic sites of postsynaptic pyramidal (Ali et al., 2008; Glykys et al., 2008; Serwanski et al., 2006). Although it has been shown that dendrite-targeting interneuron populations elicit α5 $GABA_AR$-mediated inhibition in pyramidal cells (Ali et al., 2008), it is unclear whether the α5 receptor subtype was expressed on inhibitory interneurons themselves. This was of particular interest, as we have shown previously, using the $APP^{NL\text{-}F/NL\text{-}F}$ *mouse,* the first β-amyloid precursor protein (*APP*) knock-in mouse AD model that is thought to be able to recapitulate the human condition more accurately (see (Sasaguri et al., 2017), that synaptic excitability is disrupted in various cortical regions, including the CA1 region (Petrache et al., 2019), and that this could be related to the alteration of three key modulatory interneuron populations namely; calretinin- (CR), cholecystokinin- (CCK), and somatostatin- (SST) expressing interneurons (Shi et al., 2019). We investigated whether these key modulatory interneurons located in CA1 stratum radiatum (SR), together with principal pyramidal cells, expressed the α5 subunit-containing $GABA_ARs$, in the $APP^{NL\text{-}F/NL\text{-}F}$model, age-matched to wild-type control mice, and then characterized the synaptic effects of our newly-developed α5 compound in these 4 sub-types of neurons.

Methods:

Δεελοπμεντ οφ α5-ΣΟΠ002

We re-synthesised 6,6-dimethyl-3-(2-hydroxyethyl) thio-1-(thiazol-2-yl)-6,7-dihydro-2-benzothiophen-4(5H)-one that has demonstrated selectivity for the benzodiazepine binding site and high negative allosteric modulation for the α5 $GABA_AR$ sub-type following its published route, from the parent compound (Atack, 2010; Sternfeld et al., 2004) to develop hybrid derivatives (parent compound, shown in Figure 1 (A)), full details of the synthetic steps are detailed in supplementary scheme 1 (B) (see also Sung, Lee, 1992). There were two main sites for modification, which we explored via replacement of the triazole moiety or the oxazole which

enabled us to explore late-stage modification in order to synthesise hybrid analogues to improve potency as a negative allosteric modulator acting on α5 $GABA_A$ Rs.

Computational Modelling

The structure of the α5 subunits contained in the A-type γ-aminobutyric acid receptor ($GABA_AR$) subtype formed by two α5, two β3 and one γ2 subunit was modelled based on the Cryo-EM structure 6A96 downloaded from the protein data bank (http://www.rcsb.org./pdb). Then, the complete $GABA_AR$ was modelled. Potential pockets that were large enough to bind the ligands were identified using the icmPocketfinder tool present in the ICM-Pro software (www.molsoft.com). The pocket selected was present at the interface of the subunits α5 and γ2 and was analogous to that which binds benzodiazepine in the $GABA_AR$, the human β3 homopentamer. (PDB id: 4COF). The volume of the pocket was 435.6$Å^3$.

The ligands were sketched using the LigEdit module and docked in the receptor using the docking module. The template-based docking protocol was used. The spatial orientation of benzodiazepine was selected as reference template to dock the compounds. Grid maps were generated around the template, which defined a binding site encompassed in a grid of 20 x 20 x 20$Å^3$. Docking was run with an effort of 5, storing all alternative conformations. A maximum of 25 docked conformations were generated. The final conformation was chosen based on strongest interaction energy. Visualisation of the docked poses was done by using ICM-Pro Molsoft molecular modelling package.

Preparation of Stable HEK293 Cell Lines expressing $GABA_ARs$

To test the target selectivity of α5-SOP002, a stable cell line of HEK293 cells expressing α5β2γ2 subunits of the $GABA_AR$ was developed using the previously established method based on antibiotic selection (Brown et al., 2016). HEK293 cells (2 × 106) were transfected using Lipofectamine LTX (catalog no. 15338-100, Invitrogen) with the α5 pcDNA3.1(+) construct, incorporating the G418 disulfate (Neomycin) resistance gene and β2 pcDNA3.1(+) construct, incorporating the Zeocin resistance gene. Cells were subsequently plated at the ratios of 1:3, 1:5, 1:7, 1:10, 1:15, and 1:20, and selected with G418 (Neomycin; catalog no. G5013, Sigma) and Zeocin (catalog no. R25001 Gibco) antibiotics (both at 800 μg/ml) until colonies were formed. After 7 days, 5–20 single colonies were selected and gradually scaled up. The clone expressing the highest level of $GABA_AR$ α5 and β2 subunits, as well as the previously established α2β2-HEK293 (Brown et al., 2016) stable cell line were further transfected with the γ2 pcDNA3.1$^{(+)}$ construct, incorporating the Hygromycin resistance gene, in order to produce triple cell lines. Expression of all three subunits was characterised by immunoblotting and immunocytochemistry. The α1β2γ2-HEK293 was characterised previously (Fuchs et al., 2013).

Experimental animals

All of the procedures in this study were carried out in accordance with the British Home Office regulations under the Animal Scientific Procedure Act 1986, under the project licence PPL: P1ADA633A held by the principal investigator, Dr. Afia Ali. All procedures were approved by both internal and external UCL ethics committees, and in accordance with the ARRIVE guide-lines for reporting experiments involving animals (McGrath et al., 2010). A total of ˜100 animals (disease model and wild-type) were used in this study. The animals had*ad-libitum* access to food and water and were reared in cages of maximum 5 inhabitants, with a day: night cycle of 12 hours: 12 hours.

The knock-in $APP^{NL\text{-}F/NL\text{-}F}$ AD mouse model was used for experiments (Saito et al., 2014), which consists of the introduction of two familial AD (FAD) mutations: KM670/671NL and I716F. The former, identified as the Swedish mutation, increases β-site cleavage of APP to produce elevated amounts of both $Aβ_{40}$and $Aβ_{42}$, whereas the latter, known as the Beyreuther/Iberian mutation, promotes γ-site cleavage at C-terminal position 42, thereby increasing the $Aβ_{42}/Aβ_{40}$ ratio in favour of the more hydrophobic $Aβ_{42}$ (Saito et al., 2014). Both features are key to the integrity of the disease phenotype. The knock-in line was crossed with C57BL/6 mice, and male$APP^{NL\text{-}F/NL\text{-}F}$ and age-matched wild-type (C57BL/6) mice from the same breeding were used as control at 9 - 18 months.

Animals were genotyped via standard polymerase chain reaction using the following four primers: 5'-ATCTCGGAAGTGAAGATG-3', 5'-TGTAGATGAGAACTTAAC-3', 5'-ATCTCGGAAGTGAATCTA-3', and 5'-CGTATAATGTATGCTATACGAAG-3' as previously described (Saito et al., 2014). Further details of rationale for selecting this mouse model can be found in Petrache et al., (2019).

Tissue collection and preparation

Rodents were anaesthetised by an intraperitoneal injection of 60 mg/kg phenobarbital and perfused transcardially with artificial cerebrospinal fluid (ACSF) containing sucrose. The level of anaesthesia was monitored using pedal and tail pinch reflexes, rate, depth and pattern of respiration through observation and colour of mucous membranes and skin. The ACSF comprised of (in mM): 248 sucrose, 3.3 KCl, 1.4 NaH_2PO_4, 2.5 $CaCl_2$, 1.2 $MgCl_2$, 25.5 $NaHCO_3$, and 15 glucose, which was bubbled with 95% O_2 and 5% CO_2. The animals were then decapitated and the brain removed and coronal sections hippocampus containing the neocortex ~ 300 μm thick – were cut in ice-cold standard ACSF using an automated vibratome (Leica, Germany). This standard ACSF contained (in mM): 121 NaCl, 2.5 KCl, 1.3 NaH_2PO_4, 2 $CaCl_2$, 1 $MgCl_2$, 20 glucose and 26 $NaHCO_3$, equilibrated with 95% O_2 and 5% CO_2. Slices were incubated in ACSF for one hour at room temperature (20–23 °C) prior to recording. Brain slices were placed in a submerged chamber and superfused with ACSF at a rate of 1–2 ml $min^{-1}$for electrophysiological recordings. For neuroanatomical studies, brains were immediately fixed after perfusion in 4% paraformaldehyde plus 0.2% picric acid in 0.1M phosphate buffer (PB) for 24 hours prior to sectioning.

In vitro **brain slice electrophysiology**

All whole-cell recordings were performed using patch electrodes made from filamented borosilicate glass capillaries (Harvard Apparatus, UK) using a laser puller (Sutter instruments, USA), with resistances of 8–11 M, and were visually aided by IR-DIC microscopy (Optizoom, Nikon, USA).

Whole-cell patch clamp recordings of HEK293 cells

Electrophysiological recordings of HEK293 cells stably expressing $GABA_A$Rs were performed in a whole-cell, current clamp mode. The chamber containing coverslips with the cell line was continuously superfused at a flow rate of 1.8 mL/min with the extracellular medium composed of 130 mM NaCl, 4 mM KCl, 10 mM Hepes, 20 mM $NaHCO_3$, 10 mM glucose, 1 mM $MgCl_2$, and 2 mM $CaCl_2$, and was equilibrated with 5% CO_2/95% O_2 and maintained at room temperature (~ 21-25 C). The electrodes were filled with an intracellular solution containing (in mM), 130 KCl, 3 NaCl, 4.5 phosphocreatine, 10 Hepes, 1 EGTA, 3.5 Na-ATP, 0.45 Na-GTP, and 2 $MgCl_2$ (adjusted to pH 7.2 with KOH, 290–300 mosmol/L), and had a final resistance of 3-8 MΩ. To test the target selectivity of α5-SOP002, the responsiveness to applied GABA was investigated and measured in HEK293 cells stably expressing either, α5β2γ2, α1β2γ2 or α2β2γ2 subunits of $GABA_A$Rs. The pharmacological properties of the expressed receptors were investigated by puffer-application of GABA (1 μM; Tocris Bioscience, UK) and subsequent bath-application of α5-SOP002 (0.5-1 μM), followed by diazepam (1 μM, Tocris Bioscience, UK). The change in membrane potential after GABA puff application response was recorded. The statistical test used was one-way ANOVA with a 95% confidence interval.

Whole-cell patch clamp of neurons in acute hippocampal brain slices

Whole-cell somatic recordings were performed using patch electrodes filled with a solution containing (in mM): 134 K gluconate, 10 HEPES, 10 phosphocreatine, 2 Na_2ATP, 0.2 Na_2GTP, and 0.2% w/v biocytin.

CA1 pyramidal cells and interneurons in SR and stratum lacunnosum moleculare were selected for recording based on the shape of their soma using video microscopy under near infrared differential interference contrast illumination. Cells were further characterised by their electrophysiological properties obtained from injecting a series of 500 ms depolarising and hyperpolarising current pulses and identified post-recording anatomically, as described previously in detail (Khan et al., 2018).

Spontaneous postsynaptic potentials were recorded from passive membrane responses and mixed spontaneous excitatory postsynaptic potentials (sEPSPs) and spontaneous inhibitory postsynaptic potentials (sIPSPs)

were collected in 60 second frame samples, repeated at 0.33 Hz. Recordings were carried out under the current clamp mode of operation (NPI SEC 05LX amplifier; NPI electronics, Germany), low pass filtered at 2 KHz and digitised at 5 KHz using a CED 1401 interface (Cambridge Electronic Design, UK). Input resistance was monitored throughout experiments by means of a hyperpolarising current step (-10 pA, 10 ms). Signal (Cambridge Electronic Design, UK) was used to acquire recordings and generate current steps. The average amplitudes of spontaneous events and their frequency was measured manually from single sweep data sets of 60 second recordings, including a total sweep range of 30-50 frames (*i.e.,* 30 – 50 minutes of recording); values below the baseline level of 0.1 mV were considered as noise, see (Ali et al., 2006) .

Paired whole-cell somatic recordings were obtained between CA1 CR interneurons in SR (for inhibitory connections). Unitary inhibitory postsynaptic potentials (IPSPs) were elicited by a depolarising current step into the presynaptic neuron (+0.05 nA, 5–10 ms) repeated at 0.33 Hz. The peak IPSP amplitudes, and width at half-amplitude measurements were obtained from averages including 100-200 unitary synaptic events.

Drugs for *in vitro* pharmacological studies on brain slices, zolpidem (Sigma, Aldrich, UK, 0.4 μM, dissolved first in ethanol to a final bath ethanol dilution of 1:20,000); α5-SOP002 (1-1.5 μM); diazepam (RBI, Poole UK; 1-2 μM, dissolved in ethanol to a final bath ethanol dilution of 1:5000) were bath-applied. The α5-SOP002 concentration used (1-1.5 μM) was within the range at which it is reported to act as an inverse agonist with efficacy selective for α5 containing $GABA_A$Rs (Dawson *et al.,* 2006). The concentration of zolpidem used produces near maximal effects on α1-containing receptors but submaximal effects on α2/3-containing receptors (K_d 0.2 μM for α1-containing receptors; 1.5 μM for α3 containing receptors (Munakata et al., 1998).

Neuroanatomical procedures and analysis

Immunofluorescence procedures, confocal image acquisition and analysis of CA1 neurons

Slices were incubated as described previously (Petrache et al. 2019), using $GABA_A$R α5 primary antibody (abcam, raised in mouse, 1:100) incubated concomitantly with the primary antibody targeting one of the following: calretinin (Swant, raised in goat, 1:1000), somatostatin (Santa Cruz Biotechnology, raised in rabbit, 1:500), cholecystokinin (Frontier Institute, raised in rabbit, 1:1000) or CaMKII-α (Invitrogen, raised in goat, 1:100). The secondary antibodies used were as follows: FITC (Sigma-Aldrich, anti-mouse, 1:200), Texas Red (Invitrogen, anti-rabbit/anti-mouse, 1:500) or Alexa Fluor 488 (Abcam, anti-goat, 1:500). The sections were counterstained with the nuclear stain, DAPI (Sigma-Aldrich, 1:1000).

Images were acquired at 63× magnification using a ZEISS LSM 880 confocal microscope and processed using Zen Black 2009. Collapsed Z-stacks were imported into Fiji (Image J) as *.tif* files and split into individual channels. If needed, the background was removed using the*Background subtraction* function in Image J. In the channel corresponding to the cell staining, the outline of the cells of interest was drawn manually to obtain regions of interest (ROIs). The*Coloc2* plugin was then used to obtain Pearson's R coefficient as a measure of colocalisation between the channels corresponding to the ROIs and to the α5 subunit, and Fisher's transformation was applied to convert the coefficients to a normal distribution. The results so obtained were then averaged separately for wild-type and$App^{NL\text{-}F/NL\text{-}F}$ animals, respectively, for each of the cells of interest. There were no age differences observed during the analysis, so the data were grouped without any age-dependent segregation, with ages from 2.5 months to 15 months.

Statistical analyses

All data values are given as the mean ± standard error of mean (SEM), unless otherwise stated. Prior to statistical analysis, normality and outlier tests were conducted. For comparisons between multiple groups of data, one-way or two-way ANOVA with a 95% confidence interval was used followed by a post-hoc Tukey's or Bonferroni's test for multiple comparisons. When making direct comparisons between two paired measurements, a paired, two-tailed Student's t-test was used.

Statistical analysis for the electrophysiology in the$APP^{NL\text{-}F/NL\text{-}F}$ model and the immunofluorescence data

was conducted using GraphPad Prism version 8.0.0 for Windows, GraphPad Software, San Diego, California USA, graphpad.

All statistical analyses were conducted using the statistical package Origin Pro 2016 SR1. Statistical significance was accepted where$p < 0.05$ (*$p < 0.05$, ** p<0.01). The *"n"* are given as the number of observations and the number of animals used, unless otherwise stated.

Results

In this study, we initially resynthesised a water soluble α5 $GABA_AR$-selective compound NAM, α5-SOP002 and determined its selectivity using HEK293 cells lines stably expressing α5β2γ2-, α2β2γ2- or α1β2γ2-$GABA_ARs$. To identify changes of the expression pattern of α5 $GABA_AR$ during a disease that is characterised by cognitive deficits, we used an AD mouse model and wild-type mice at 10-12 months, when the typical hallmarks of AD in the hippocampus are present, including synaptic loss, accumulation of amyloid-β (Aβ) and proliferation of reactive astrocytes and microglia (Petrache et al., 2019; Saito et al., 2014). The effects of α5-SOP002 on inhibitory synaptic potentials recorded in the identified cells that co-expressed α5 $GABA_AR$ were investigated.

The development of the α5-SOP002

compound

We initially developed four hybrid analogues of this compound with an array of biological activity ranging from inactive controls to highly potent derivatives resulting in, α5-SOP002 (Figure 1 A-C, see also supplementary scheme 1).

The structure of the α5 subunits contained in the α5 $GABA_AR$ was modelled and later used to generate the $GABA_AR$ subtype containing two α5, two β3 and one γ2 subunits. Once a reliable model was obtained, our key compound, α5-SOP002 was docked into the interface of subunit α5 (Figure 1 (D-H)) and subunit γ2, obtaining the best binding mode with a VlsScore of -20.35.

Overall, α5-SOP002 indicated good aqueous solubility and good blood-brain barrier penetration as evidenced from the spatial memory recall experiments in rats following intraperitoneal injection (i.p.) (supplementary Figure 1). The supplementary section, which compares*in vivo* spatial memory tests (Becker et al., 1980) and *in vitro* paired whole recording data from 25-28 day old rats using α5-SOP002 and the published analogue L-655,708 (a similar compound to α5IA originally developed by Merck Sharp and Dome (UK) and available from Tocris (UK) were discribed. *In vivo* , spatial memory recall experiments were not repeated in the mouse lines due to the conclusions reached from the results (see below).

α5-ΣΟΠ002 σελεςτιελψ ταργετς α5 συβυνιτς οφ ΓΑΒΑ$_A$Ρς

An α5β2γ2-HEK293 cell line was developed to investigate the selectively of α5-SOP002 towards the α5-containing $GABA_ARs$. The cell surface expression of all three $GABA_AR$ subunits in this cell line was characterised using immunocytochemistry (Figure 2 (A)) with subunit-specific antibodies. The responsiveness of the α5β2γ2-HEK293 stable cell line to GABA and diazepam demonstrated the presence of functional α5β2γ2-$GABA_ARs$ at the cell surface (Figure 2 (D)), while application of α5-SOP002, immediately following GABA, confirmed its activity as a negative allosteric modulator (*i.e.* inverse agonist) of these receptors. These experiments were repeated using the α1β2γ2-HEK293 and α2β2γ2-HEK293 stable cell lines in order to test the specificity of α5-SOP002. The cell surface expression of α1β2γ2-and α2β2γ2-$GABA_ARs$ was also demonstrated using immunocytochemistry with subunit-specific antibodies (Figure 2 (B-C)), as shown previously (Brown et al., 2016; Fuchs et al., 2013).

HEK293 cells expressing α5β2γ2-$GABA_ARs$ responded to GABA (10 μM), puff-applied (5 s) in close proximity, with a large hyperpolarisation, recorded at a membrane holding potential of -60 mV. This was also recorded in the α1β2γ2-HEK293 and α2β2-HEK293 stable cell lines (Figure 2 (E-F)).

The response of the three cell lines to GABA was measured and the changes of the response after bath-application of 1 μM α5-SOP002 followed by puff-application of the broad spectrum $GABA_AR$ modulator, diazepam (1 μM) was also analysed (Figure 2 (D-F)).

Bath-application of α5-SOP002 (1 μM) significantly reduced the hyperpolarising GABA inhibitory response in cells expressing α5β2γ2- $GABA_ARs$ (mean ± SEM: control GABA: 10.0 ± 5.0 mV; α5-SOP002: 5.12 ± 2.2 mV; P <0.05, n = 8), while puff-application of diazepam had an opposite effect leading to a significant enhancement of GABA response (12.26 ± 6.94, P<0.05, n= 8, one-way ANOVA, Figure 2 (G)). In contrast, there were no significant changes in the GABA response in the presence of α5-SOP002 in cells expressing α1β2γ2-$GABA_ARs$ (control GABA: 18.0 ± 5.0 mV; α5-SOP002: 18.0 ± 4.5, n =6; Figure 2 (E)) or α2β2γ2-HEK293 (control GABA: 13.5 ± 11.5 mV; α5-SOP002: 13.0 ± 10.5 mV,n =6; Figure 2 (F)). Puff-application of diazepam nevertheless significantly enhanced the hyperpolarising inhibitory GABA response in both, α1β2γ2-HEK293 (24.0 ± 7.6 mV, P <0.01, n=6) and α2β2γ2-HEK293 cells (17.0 ± 12.0, P <0.05,n= 6) (Figure 2 (H-I)). This confirmed the selectivity of α5-SOP002 towards $GABA_ARs$ containing the α5 subunit.

Πρεσερατιον οφ α5 ΓΑΒΑ$_A$Ρς ιν ΄Α1 πψραμιδαλ ςελλς ανδ 3 συβ-τψπες οφ ιντερνευρονς ιν τηε ΑΔ μοδελ

Using immunofluorescence and confocal microscopy analysis in the CA1 region of the hippocampus, we investigated α5 subunit-containing $GABA_AR$ expression in three sub-types of modulatory inhibitory interneurons, CR-, SST- and CCK-expressing interneurons, as well as in pyramidal cells (stained for CaMKII-α) in the$APP^{NL\text{-}F/NL\text{-}F}$ mouse model and wild-type animals (Figure 3(A-D)). The imaged area in each case is shown in Figure 3(E).

This was measures in three different ways, quantification of the total intensity of α5 signal in CA1 measured from confocal Z-stacks, followed by the quantification of α5 expression from individual cell populations measured from their somata and dendrites, using Pearson's correlation coefficient R with Fisher's transformation.

We also quantified the total intensity of α5 signal in CA1 confocal Z-stacks and observed no differences in the AD model compared to wild-type (P > 0.05, n =5 wild-type animals and 6 $APP^{NL\text{-}F/NL\text{-}F}$ animals), suggesting a preservation of α5 expression in the$APP^{NL\text{-}F/NL\text{-}F}$ animals.

The α5 subunits expressed on all three interneuron subtypes were analysed further from somata of the different cell types (Figure 3 (F)). There was no significant change in α5 expression on CR cells in$APP^{NL\text{-}F/NL\text{-}F}$ animals compared to wild-type (only a slight increase of 11.86 ± 3.14 %, P > 0.05, n =6 wild-type animals and 7$APP^{NL\text{-}F/NL\text{-}F}$ animals). Similarly, there was no change in the expression of α5 expression in SST or CCK interneurons between wild-type and $APP^{NL\text{-}F/NL\text{-}F}$ mice (only insignificant changes of; 27.35 ± 12.61 % and 36.09 ± 12.45 % observed in SST and CCK cells, respectively, in$APP^{NL\text{-}F/NL\text{-}F}$ animals compared to wild-type animals, P > 0.05, n =6). Thus, the three interneuron subtypes studies showed no significant differences in α5 subunit expression between wild-type animals and$APP^{NL\text{-}F/NL\text{-}F}$ animals, highlighting a preservation of the α5 subunit in AD.

Analysis of CaMKII-α and α5 co-staining (Figure 3 (F)) showed no significant differences in the expression of α5 expression on the pyramidal cells in $APP^{NL\text{-}F/NL\text{-}F}$ animals compared to wild-type (P > 0.05, n =5). This observation is consistent with previous studies, which reported α5 expression on pyramidal cells (Brünig et al, 2002).

Next, we investigated the expression of the α5 subunit on CR, SST, and pyramidal cell dendrites (Figure 3 (G)), as the subunit has been reported to be located postsynaptically at dendritic sites where presynaptic CR cells target SST interneurons (Magnin et al., 2019) and on postsynaptic dendrites of pyramidal cells (Ali and Thomson, 2008). CCK cells also receive input-from dendrite-targeting interneurons (Ali, 2007), but their dendrites could not be investigated in detail here, due to the unavailability of specific anti-CCK anitbody that shows good expression of CCK in dendrites in mouse tissue. We investigated up to 5 cells in each animal, and observed no significant difference in the α5 expression between the genotypes or neuron subtypes in their dendrites (P > 0.05, one-way ANOVA with post-hoc Tukey's test for multiple comparisons).

α5-ΣΟΠ002 'νορμαλισεσ' ˜P ιντερνευρον αβερραντ ινηιβιτιον οβσερεδ ιν ΑΔ

Inhibition recorded from spontaneous synaptic events

The effect of α5-SOP002 at inhibitory CR interneurons was determined on brain slices by performing whole-cell recordings under current clamp mode. Spontaneous inhibitory postsynaptic potentials (sIPSPs) and spontaneous excitatory postsynaptic potentials (sEPSPs) were recorded from CR interneurons at 10-12 months old wild-type and$App^{NL\text{-}F/NL\text{-}F}$ mice at holding membrane potentials of -60mV (to observe both excitation and inhibition, Figure 4 (A-D)), the average data are shown in Table 1. The average peak frequency and amplitude of sIPSPs significantly increased in the AD model compared to wild-type age-matched mice at -60 mV, was consistent with our previous publication that reported this interesting abnormal observation in the CR cells (Shi et al., 2019). In the$App^{NL\text{-}F/NL\text{-}F}$ mice sIPSP frequency and amplitude was abnormally higher by 93.4 ± 7.5 % (P <0.01,n =5, unpaired, two-tailed Student's t-test) and 55.6 ± 23.3 % (P <0.01, n =5, unpaired, two-tailed Student's t-test) of control sIPSPs recorded in age-matched wild-type mice, respectively (Figure 4 (C)).

Bath-application of α5-SOP002 (1 μM) reduced the sIPSP frequency and amplitude in both wild-type and $App^{NL\text{-}F/NL\text{-}F}$mice (see Table 1 for details). The significantly reduced sIPSP frequency (48 ± 3.2 %, P <0.01, n =5, one-way ANOVA with post-hoc Bonferroni's test) and amplitude (56.3 ± 5.7 %,P <0.01, n =5, one-way ANOVA with post-hoc Bonferroni's test) recorded in CR cells from$App^{NL\text{-}F/NL\text{-}F}$ mice was comparable to the control CR cells recorded in age-matched wild-type mice. The average sEPSP frequency and amplitude also changed, but the slight increase was not significantly different from control mean (Figure 4 (D), Table 1).

Interestingly, in the $App^{NL\text{-}F/NL\text{-}F}$ mice, bath-application of α5-SOP002 also caused an average ˜5 mV depolarisation of the cell membrane, suggesting a reduction in tonic inhibition.

Unitary inhibition recorded from two synaptically-connected CR cells

CR interneurons during the late stages of AD were readily identifiable under ID-DIC during experiments, (in striking contrast to CCK or SST cells that were not easily visualised), allowing us to perform paired recording between two CR cells. We performed paired recording in the$App^{NL\text{-}F/NL\text{-}F}$ animals only due to the very technically challenging nature of these experiments, hampered by the age of the mice. However, supplementary Figure 1(E-F) shows examples of paired recordings performed in young healthy control rodents.

Consistent with the finding that the sIPSPs recorded in CR cells were sensitive to α5-SOP002, unitary IPSPs recorded between two CR cells in SR were also reduced in peak amplitude and width at half amplitude following bath-application of α5-SOP002 at -55mV (Figure 4E). The decrease in amplitude and width was: 51.20 ± 7.36 % (P <0.05, n =3, paired, two-tailed Student's t-test) and 28.25 ± 1.02 % (P <0.01, n =3, paired, two-tailed Student's t-test) of control IPSPs recorded in$App^{NL\text{-}F/NL\text{-}F}$, respectively. Bath-application of the α1 subunit-selective agonist, zolpidem did not change the IPSP properties at these synapses, which was consistent with previous studies that reported insensitivity to zolpidem at synapses involving presynaptic dendrite-preferring cells (Ali et al., 2008). Subsequent addition of the broad spectrum benzodiazepine site agonist, diazepam (after α5-SOP002) enhanced IPSP amplitude by 186.59 ± 41.45 % (P <0.05, n =3, one-way ANOVA) and width at half amplitude by, 37.31 ± 6.71 % (P >0.05, n =3, one-way ANOVA with post-hoc Bonferroni's test) of control IPSPs recorded in $App^{NL\text{-}F/NL\text{-}F}$ mice (Figure. 4 (E-F)).

The recorded (putative) CR –expressing interneurons, recovered post-hoc were usually oval with 2-3 vertically orientated primary beaded dendrites, usually from opposite poles, with fine axons containing small/medium sized boutons originated from the soma or a primary dendrite and ramified quite sparsely in mid-SR, as described previously (Shi et al., 2019) These cells resembled previously published CR cells (Gulyas et al., 1996).

α5-ΣΟΠ002 ρεδυςεδ ινηιβιτιον, βυτ εξαςερβατεδ σψναπτις ηψπερεξςιταβιλιτψ ατ ˜˜K ανδ πρινςιπαλ ςελλς

We then attempted to record from CCK and pyramidal cells in CA1. The anatomically recovered interneurons resembled the most abundant sub-type of CCK-expressing cells, the Schaffer collateral-associated (SCA) interneuron with soma/dendrites and axons of these interneurons are predominantly located in the SR and axonal branches predominantly ramifying in SR (Ali, 2007). CCK and SST-expressing cells in aged AD mice decline in densities during the pathogenesis of AD (Shi et al., 2019), which hampered the yield of the recordings. Furthermore, we could not record from SST-expressing cells in stratum oriens due to their sparse appearance in the slices and the heavy myelination in this region at 10-12 months of age.

The $GABA_AR$ α5 NAM, α5-SOP002, reduced the average sIPSP amplitude and frequency of both CCK-SCA and pyramidal cells in age-matched wild-type and $APP^{NL\text{-}F/NL\text{-}F}$ mice (Figure 5, see Table 1 for detailed values). In$APP^{NL\text{-}F/NL\text{-}F}$ mice, the average sIPSP frequency and amplitude recorded at CCK-SCA cells reduced by 45.80 ± 10.40 % and 53.0 ± 7.5 %, of control values by bath- application of α5-SOP002, ($P <$ 0.05 for frequency and, $P < 0.01$ for amplitude, one-way ANOVA , with post-hoc Tukey's test, n= 3, Figure 5(A-B) and (E-F)). Similarly, in$App^{NL\text{-}F/NL\text{-}F}$ mice sIPSP frequency and amplitude recorded in pyramidal cells reduced following bath-application α5-SOP002, by 16.50 ± 0.91 % ($P > 0.05$, n =5, one-way ANOVA) and 49.17 ± 7.69% (P <0.001, n =5, one-way ANOVA with post-hoc Tukey's test) of control sIPSPs recorded in age-matched wild-type mice, respectively (Figure 5 (D-E) and (G-H)).

However, in contrast, with bath-application of α5-SOP002, the sEPSP properties recorded in CCK-SCA and pyramidal cells *increased* in both wild-type and $App^{NL\text{-}F/NL\text{-}F}$ mice (See Table 1). These cells recorded in the AD model displayed an abnormal level of hyperexcitation and a deficit in inhibition compared to the healthy, wild-type mice (Figure 5 (G-H)) (see also (Petrache et al., 2019; Shi et al., 2019), which was further exacerbated when challenged with the $GABA_AR$ α5 NAM, α5-SOP002. With bath application of α5-SOP002, in the $APP^{NL\text{-}F/NL\text{-}F}$ mice, the increase in sEPSP frequency and amplitude in CCK-SCA was, 42 ± 2.26 % and 114 ± 9.04 % (P <0.05 (Frequency),P <0.01 (amplitude), n =3, one-way ANOVA), and in pyramidal cells was, 32.48 ± 0.94 % and 48.0 ± 3.42 % (P <0.01, n =5, one-way ANOVA), respectively.

Discussion

In this study, we have focused on establishing whether the modulation of α5 $GABA_AR$-associated synaptic transmission by compounds with negative allosteric effects could be a successful targeted therapeutic strategy in Alzheimer's disease (AD).

It has been evidenced that the $GABA_AR$ α subunits form a structural basis for the different pharmacological and thus, behavioural profiles of various allosteric modulators of these receptors (Mohler et al., 2002; Whiting, 2003). In particular, allosteric modulation of α5-containing $GABA_ARs$ has been shown to gate the acquisition and modify the extinction of associative learning in animal models (Collinson et al., 2002; Crestani et al., 2002; Dawson et al., 2006; Yee et al., 2004), yet clinical trials aimed at alleviating cognitive deficits with selective negative allosteric modulators of these receptors have failed. Our objective in the current study was to resynthesize a hybrid compound of an established NAM, 6,6-dimethyl-3-(2-hydroxyethyl)thio-1-(thiazol-2-yl)-6,7-dihydro-2-benzothiophen-4(5H)-one, in order to increase its' aqueous solubility, as well as its' selectivity and potency as a negative allosteric modulator of α5 $GABA_ARs$. Inhibition mediated via these receptors is widespread in the brain but it is particularly abundant in the hippocampus (Magnin et al., 2019), where we have identified four sub-populations of neurons that express high levels of α5 $GABA_ARs$. Using the $App^{NL\text{-}F/NL\text{-}F}$knock-in mouse model of AD, that shows an age-dependent increase in the main pathological hallmarks of this disease, including accumulation of Aβ, activation of microglia and reactive astrocytes and neurodegeneration (Shi et al., 2019), we have revealed how the negative allosteric modulation of α5 $GABA_ARs$ can*exacerbate* the aberrant hyperexcitability and synaptic dysregulation in AD.

Mechanism of action of our key compound α5-SOP002

From computational modelling, we showed that α5-SOP002 docked into the interface of the α5 and γ2 subunits, indicating that it works via the benzodiazepine binding site (composed of a γ2 and either α1, α2, α3 or an α5 subunit of the $GABA_AR$). Normally, binding of benzodiazepines to these sites causes a conformational change of the receptor increasing the receptor's affinity for GABA, resulting in an enhanced

inhibitory (hyperpolarising) effect mediated via Cl^- flux (Sieghart, 1995). However, NAMs, such as α5-SOP002, when bound to the same $GABA_AR$ sub-types *decrease* the influx of Cl^- which leads to depolarisation of the membrane and a *decreased* net inhibitory effect (Haefely et al., 1993). The data obtained from various HEK cell-lines constructed to contain specific $GABA_AR$ subunits and electrophysiological recordings performed, provided evidence to suggest that the developed compound, α5-SOP0002 specifically acted as a negative allosteric modulator at α5 $GABA_ARs$ and had no effect on α1 or α2 subunit-containing $GABA_ARs$. However, this does not preclude an action of α5-SOP0002 as a NAM in native $GABA_ARs$ where the synaptic colocalisation of the α subunits could result from a combination of the insertion of either two identical α subunits, or from insertion of a single receptor sub-type that contains two different α subunits. The α subunit that is adjacent to the γ2 subunit dominates the pharmacological profile of the receptor as suggested previously by binding studies on double immunopurified α1/α5 $GABA_ARs$ (Araujo et al., 1999). Thus, we suggest that α5-SOP002 acts by specifically binding at the interface of α5 and γ2 subunits, which determines a unique pharmacological profile of this compound.

Πρεσερατιον οφ α5 ΓΑΒΑ$_A$Ρς ιν ̂A1 ιν τηε αγεδ μουσε μοδελ οφ ΑΔ

We show for the first time, that the α5 $GABA_ARs$ in the CA1 region of the hippocampus are expressed on CR- expressing interneurons, specialised for dis-inhibition, but also SST- and CCK- expressing interneurons, specialised for fine-tuning pyramidal cell activity. The rationale for selecting CCK- and SST- expressing cells in our experiments stems from previous studies showing that dendrite-targeting interneurons form synapses with the pyramidal cells that incorporate the α5 subunit-containing $GABA_ARs$ (Ali et al., 2008). However, in the current study, we show that SST- and CCK- expressing cells are also recipients of postsynaptic inhibition mediated by α5 $GABA_ARs$.

Our findings corroborate previous studies that have demonstrated that α5 $GABA_ARs$ are preserved in post-mortem tissue obtained from AD patients (Howell et al., 2000), but also studies showing expression of α5 $GABA_ARs$ in pyramidal cells (Brunig et al., 2002). Our experiments demonstrate expression of these receptors on the soma of CR, SST and CCK interneurons in addition to pyramidal cells. Since SST and CCK cells decline in disease (Shi et al., 2019), this distribution could be due to a subgroup of SST interneurons compensating for the reduction in numbers by upregulating α5 $GABA_AR$ expression. Given that both CCK and SST cells are hyperactive in AD (Shi et al., 2019; Zhang et al., 2016), it is possible that α5 expression represents a compensatory mechanism.

Investigation into the levels of α5 expression on dendrites showed larger variability, notable being the level of expression on SST interneurons in the $App^{NL\text{-}F/NL\text{-}F}$ mice, which could be linked to the differential input those cells receive. Similarly, pyramidal cells showed larger variability, and we propose that this is input-dependent. Earlier studies investigating regulation of $GABA_AR$ surface expression show that, during seizures, receptors can be rapidly internalised leading to increased neuronal activity (Goodkin et al., 2007). A similar mechanism could be taking place in AD, contributing to the abnormal inhibitory-excitatory balance that characterises this disease (Petrache et al., 2019).

Αβερραντ ινηιβιτιον ιν ̂P ιντερνευρονς ις ‘νορμαλισεδ’ βψ α5-ΣΟΠ002 ιν τηε ΑΔ μοδελ

Previously, we reported that the CR interneuron network was “preserved” in our AD model following post-phenotypic changes such as increased Aβ accumulation and proliferation of microglial cells and astrocytes, which is consistent with anatomical studies reporting resilience of CR cells in post-mortem brains of AD patients (Fonseca et al., 1995). Using our key NAM molecule, α5-SOP002, we have demonstrated that abnormal synaptic inhibition received by CR interneurons in the $App^{NL\text{-}F/NL\text{-}F}$ mouse model “normalized” to control levels. Moreover, paired whole-cell recordings revealed that α5-SOP002 had a pronounced effect at synapses between interneurons compared to synapses received by pyramidal cells, therefore impacting on dis-inhibition in the hippocampal CA1 region. This is important, given that we have previously demonstrated a gradual decline in the number of CCK- and SST-inhibitory interneurons in our AD model, suggesting an overall reduction in their inhibitory function, which was in stark contrast to the density of CR cells (Shi et al., 2019).

The sIPSPs recorded in this study are most likely due to the activation of synaptic α5 $GABA_A$Rs, since we did not observe any significant change in either membrane potential or input resistance associated with the application of α5-SOP002 onto CR interneurons (or neither CCK nor pyramidal cells) . We suggest that in the CR interneuron network, showing zolpidem insensitivity, augmentation by diazepam and depression by α5-SOP002, the α5 subunit may coexist with another α5 subunit or either α2 or α3- subunit, where α5 pharmacology predominates.

However, interestingly, we observed a small positive (depolarisation) change in membrane potential in CR interneurons with α5-SOP002 in the AD model only, suggesting that these cells maybe in a state of excess tonic inhibition in the disease state. We suggest that the release from the abnormal tonic inhibition at CR cells, indicated by the depolarisation of the membrane potential, could be caused by negative allosteric modulation of extrasynaptic α5-receptors (Caraiscos et al., 2004; Magnin et al., 2019), which are tonically active due to increased levels of ambient GABA (Scimemi et al., 2005). Given that α5-SOP002 requires the presence of α- and γ-subunits, it is unlikely that it can affect the activity of other types of extrasynaptic $GABA_A$Rs such as those containing the δ-subunit. However, the contribution of extrasynaptic α5 $GABA_A$Rs to the CR interneuron network remains to be fully investigated.

Negative allosteric modulation of α5 subunit-containing $GABA_A$Rs further exacerbates hyperexcited synapses in the AD model

As previously described, there is a gradual decline in the number of CCK-SCA interneurons and CaMKII-expressing pyramidal cells in aged AD mice, with the later showing hyperexcitability when the pathological hallmarks of AD were present, clearly indicating the abnormalities in neuronal network activity (Shi et al., 2019). Since these cells express the α5 subunit, it is not surprising that α5-SOP002 can reduce inhibition at CCK and pyramidal cells, and therefore exacerbate imbalance between the excitation and inhibition at these key neuronal populations in CA1 and impact on the efficacy and precision of the fine-tuning inhibition at both temporal and spatial domains. These are reasonable assumptions, since; CCK-SCA cells, which are ideally positioned to modulate CA3 input, (Iball et al., 2011), and are important for fine-tuning individual neurons by retrograde cannabinoid signalling (Ali, 2007; Katona et al., 1999), whereas the SST, that fine-tune distal inputs received by CA1 pyramidal cells (Leao et al., 2012; Magnin et al., 2019), and are important for coordinating neuronal assemblies and gating of memory formation (Cutsuridis et al., 2009; Tort et al., 2007). Due to the prime location of these interneurons, it is feasible to suggest that both of these interneuron sub-populations may be involved in routing information flow to CA1 from CA3 and entorhinal cortex- pathways that are important for memory acquisition and retrieval, and their destruction during the pathogenesis of AD may be a significant contributing factor to cognitive decline. This is further supported by recent studies that show SST interneuron dysfunction triggered by amyloid β oligomers underlies hippocampal oscillation important for memory functions (Chung et al., 2020).

Conclusion

In summary, using a multi-disciplinary approach, we have developed a novel, selective negative allosteric modulator for α5 $GABA_A$Rs and characterised its effects on hippocampal dis-inhibition in a well-established mouse model of AD. We have shown that this modulator can "normalise" abnormal, inhibitory synaptic activity received by CR interneurons in this model, suggesting initially its' therapeutic potential. Furthermore, our data provides evidence that α5 $GABA_A$Rs are also preserved in other types of interneurons, such as CCK, SST and CR interneurons.

Since our data suggest that α5 $GABA_A$Rs are widely expressed by both dysfunctional and resilient neurons, and also that α5-SOP002 can compromise further the aberrant hyperexcitable network in the AD model, we propose that pharmacological modulation of α5 subunit-containing $GABA_A$R networks may not be a suitable therapeutic target for cognitive impairment in AD. Although the evidence suggests an overall improvement of memory with $GABA_A$ α5 inverse agonists in rodents, it is yet to be established what kind of short- and long-term effects these compounds might have in patients. We propose that the lack of specificity and efficacy in clinical trials could be at least in part due to a wide expression of α5 $GABA_A$Rs in the hippocampus, both

by various types of interneurons and pyramidal cells. Thus, targeting the α5 subunit with NAMs would result in a global effect on the hippocampal networks and would lack the specificity required to restore the complex network alteration during pathogenesis of AD that leads to the observed excitatory-inhibitory imbalance.

References

Ali AB (2007). Presynaptic Inhibition of GABAA receptor-mediated unitary IPSPs by cannabinoid receptors at synapses between CCK-positive interneurons in rat hippocampus. Journal of neurophysiology 98**:**861-869.

Ali AB*, et al.* (2006). Distinct Ca2+ channels mediate transmitter release at excitatory synapses displaying different dynamic properties in rat neocortex. Cerebral cortex 16**:** 386-393.

Ali AB*, et al.* (2008). Synaptic alpha 5 subunit-containing GABAA receptors mediate IPSPs elicited by dendrite-preferring cells in rat neocortex. Cerebral cortex 18**:** 1260-1271.

Araujo F*, et al.* (1999). Native gamma-aminobutyric acid type A receptors from rat hippocampus, containing both alpha 1 and alpha 5 subunits, exhibit a single benzodiazepine binding site with alpha 5 pharmacological properties. The Journal of pharmacology and experimental therapeutics 290**:** 989-997.

Atack JR (2010). Preclinical and clinical pharmacology of the GABAA receptor alpha5 subtype-selective inverse agonist alpha5IA. Pharmacology & therapeutics 125**:** 11-26.

Atack JR*, et al.* (2006). L-655,708 enhances cognition in rats but is not proconvulsant at a dose selective for alpha5-containing GABAA receptors. Neuropharmacology 51**:** 1023-1029.

Atack JR*, et al.* (2009). In vitro and in vivo properties of 3-tert-butyl-7-(5-methylisoxazol-3-yl)-2-(1-methyl-1H-1,2,4-triazol-5-ylmethoxy)- pyrazolo[1,5-d]-[1,2,4]triazine (MRK-016), a GABAA receptor alpha5 subtype-selective inverse agonist. The Journal of pharmacology and experimental therapeutics 331**:** 470-484.

Ballard TM*, et al.* (2009). RO4938581, a novel cognitive enhancer acting at GABAA alpha5 subunit-containing receptors. Psychopharmacology 202**:** 207-223.

Becker JT*, et al.* (1980). Neuroanatomical bases of spatial memory. Brain research 200**:** 307-320.

Braudeau J*, et al.* (2011). Specific targeting of the GABA-A receptor alpha5 subtype by a selective inverse agonist restores cognitive deficits in Down syndrome mice. J Psychopharmacol 25**:**1030-1042.

Brown LE*, et al.* (2016). gamma-Aminobutyric Acid Type A (GABAA) Receptor Subunits Play a Direct Structural Role in Synaptic Contact Formation via Their N-terminal Extracellular Domains. J Biol Chem 291**:** 13926-13942.

Brunig I*, et al.* (2002). Intact sorting, targeting, and clustering of gamma-aminobutyric acid A receptor subtypes in hippocampal neurons in vitro. J Comp Neurol 443**:** 43-55.

Caraiscos VB*, et al.* (2004). Tonic inhibition in mouse hippocampal CA1 pyramidal neurons is mediated by alpha5 subunit-containing gamma-aminobutyric acid type A receptors. Proceedings of the National Academy of Sciences of the United States of America 101**:** 3662-3667.

Chambers MS*, et al.* (2003). Identification of a novel, selective GABA(A) alpha5 receptor inverse agonist which enhances cognition. Journal of medicinal chemistry 46**:** 2227-2240.

Chung H*, et al.* (2020). Dissociation of somatostatin and parvalbumin interneurons circuit dysfunctions underlying hippocampal theta and gamma oscillations impaired by amyloid beta oligomers in vivo. Brain Struct Funct 225**:** 935-954.

Collinson N*, et al.* (2006). An inverse agonist selective for alpha5 subunit-containing GABAA receptors improves encoding and recall but not consolidation in the Morris water maze. Psychopharmacology 188**:** 619-628.

Collinson N, *et al.* (2002). Enhanced learning and memory and altered GABAergic synaptic transmission in mice lacking the alpha 5 subunit of the GABAA receptor. The Journal of neuroscience : the official journal of the Society for Neuroscience 22**:** 5572-5580.

Crestani F, *et al.* (2002). Trace fear conditioning involves hippocampal alpha5 GABA(A) receptors. Proceedings of the National Academy of Sciences of the United States of America 99**:**8980-8985.

Cutsuridis V, *et al.* (2009). Hippocampus, microcircuits and associative memory. Neural Netw 22**:** 1120-1128.

Dawson GR, *et al.* (2006). An inverse agonist selective for alpha5 subunit-containing GABAA receptors enhances cognition. The Journal of pharmacology and experimental therapeutics 316**:** 1335-1345.

Duchon JM, *et al.* (2019). Safety and Varicella Outcomes in In Utero-Exposed Newborns and Preterm Infants Treated With Varicella Zoster Immune Globulin (VARIZIG): A Subgroup Analysis of an Expanded-Access Program. J Pediatric Infect Dis Soc.

Eimerbrink MJ, *et al.* (2019). The alpha5-GABAAR inverse agonist MRK-016 upregulates hippocampal BDNF expression and prevents cognitive deficits in LPS-treated mice, despite elevations in hippocampal Abeta. Behav Brain Res 359**:** 871-877.

Fonseca M, *et al.* (1995). Calretinin-immunoreactive neurons in the normal human temporal cortex and in Alzheimer's disease. Brain research 691**:** 83-91.

Fuchs C, *et al.* (2013). GABA(A) receptors can initiate the formation of functional inhibitory GABAergic synapses. Eur J Neurosci 38**:** 3146-3158.

Ghafari M, *et al.* (2017). Formation of GABAA receptor complexes containing alpha1 and alpha5 subunits is paralleling a multiple T-maze learning task in mice. Brain Struct Funct 222**:** 549-561.

Glykys J, *et al.* (2008). Which GABA(A) receptor subunits are necessary for tonic inhibition in the hippocampus? The Journal of neuroscience : the official journal of the Society for Neuroscience 28**:** 1421-1426.

Goodkin HP, *et al.* (2007). GABA(A) receptor internalization during seizures. Epilepsia 48 Suppl 5**:** 109-113.

Gulyas AI, *et al.* (1996). Interneurons containing calretinin are specialized to control other interneurons in the rat hippocampus. The Journal of neuroscience : the official journal of the Society for Neuroscience 16**:** 3397-3411.

Haefely WE, *et al.* (1993). The multiplicity of actions of benzodiazepine receptor ligands. Canadian journal of psychiatry Revue canadienne de psychiatrie 38 Suppl 4**:** S102-108.

Howell O, *et al.* (2000). Density and pharmacology of alpha5 subunit-containing GABA(A) receptors are preserved in hippocampus of Alzheimer's disease patients. Neuroscience 98**:** 669-675.

Iball J, *et al.* (2011). Endocannabinoid Release Modulates Electrical Coupling between CCK Cells Connected via Chemical and Electrical Synapses in CA1. Frontiers in neural circuits 5**:** 17.

Katona I, *et al.* (1999). Postsynaptic targets of somatostatin-immunoreactive interneurons in the rat hippocampus. Neuroscience 88**:** 37-55.

Khan AA, *et al.* (2018). Cannabidiol exerts antiepileptic effects by restoring hippocampal interneuron functions in a temporal lobe epilepsy model. Br J Pharmacol.

Leao RN, *et al.* (2012). OLM interneurons differentially modulate CA3 and entorhinal inputs to hippocampal CA1 neurons. Nature neuroscience 15**:** 1524-1530.

Liu R, *et al.* (1996). Synthesis and pharmacological properties of novel 8-substituted imidazobenzodiazepines: high-affinity, selective probes for alpha 5-containing GABAA receptors. Journal of medicinal chemistry 39**:** 1928-1934.

Magnin E, *et al.* (2019). Input-Specific Synaptic Location and Function of the alpha5 GABAA Receptor Subunit in the Mouse CA1 Hippocampal Neurons. The Journal of neuroscience : the official journal of the Society for Neuroscience 39**:** 788-801.

Martinez-Cue C, *et al.* (2014). Treating enhanced GABAergic inhibition in Down syndrome: use of GABA alpha5-selective inverse agonists. Neurosci Biobehav Rev 46 Pt 2**:** 218-227.

McGrath JC, *et al.* (2010). Guidelines for reporting experiments involving animals: the ARRIVE guidelines. Br J Pharmacol 160**:**1573-1576.

McKernan RM, *et al.* (1996). Which GABAA-receptor subtypes really occur in the brain? Trends Neurosci 19**:** 139-143.

Mohler H, *et al.* (2002). A new benzodiazepine pharmacology. The Journal of pharmacology and experimental therapeutics 300**:** 2-8.

Munakata M, *et al.* (1998). Temperature-dependent effect of zolpidem on the GABAA receptor-mediated response at recombinant human GABAA receptor subtypes. Brain research 807**:** 199-202.

Petrache AL, *et al.* (2019). Aberrant Excitatory-Inhibitory Synaptic Mechanisms in Entorhinal Cortex Microcircuits During the Pathogenesis of Alzheimer's Disease. Cerebral cortex 29**:**1834-1850.

Price JL, *et al.* (2001). Neuron number in the entorhinal cortex and CA1 in preclinical Alzheimer disease. Arch Neurol 58**:**1395-1402.

Quirk K, *et al.* (1996). [3H]L-655,708, a novel ligand selective for the benzodiazepine site of GABAA receptors which contain the alpha 5 subunit. Neuropharmacology 35**:** 1331-1335.

Rissman RA, *et al.* (2007). GABA(A) receptors in aging and Alzheimer's disease. J Neurochem 103**:** 1285-1292.

Roche clinical trial for Basmisanil (RO5186582) started in 2016 and finished in 2019, Clinical Trials US website https://clinicaltrials.gov/ct2/show/NCT02953639

Saito T, *et al.* (2014). Single App knock-in mouse models of Alzheimer's disease. Nature neuroscience 17**:** 661-663.

Sasaguri H, *et al.* (2017). APP mouse models for Alzheimer's disease preclinical studies. EMBO J 36**:** 2473-2487.

Savic MM, *et al.* (2008). PWZ-029, a compound with moderate inverse agonist functional selectivity at GABA(A) receptors containing alpha5 subunits, improves passive, but not active, avoidance learning in rats. Brain research 1208**:** 150-159.

Scimemi A, *et al.* (2005). Multiple and plastic receptors mediate tonic GABAA receptor currents in the hippocampus. The Journal of neuroscience : the official journal of the Society for Neuroscience 25**:** 10016-10024.

Serwanski DR, *et al.* (2006). Synaptic and nonsynaptic localization of GABAA receptors containing the alpha5 subunit in the rat brain. J Comp Neurol 499**:** 458-470.

Shi A, *et al.* (2019). Preserved Calretinin Interneurons in an App Model of Alzheimer's Disease Disrupt Hippocampal Inhibition via Upregulated P2Y1 Purinoreceptors. Cerebral cortex.

Sieghart W (1995). Structure and pharmacology of gamma-aminobutyric acidA receptor subtypes. Pharmacological reviews 47**:** 181-234.

Sieghart W, *et al.* (2002). Subunit composition, distribution and function of GABA(A) receptor subtypes. Curr Top Med Chem 2**:**795-816.

Sternfeld F, *et al.* (2004). Selective, orally active gamma-aminobutyric acidA alpha5 receptor inverse agonists as cognition enhancers. Journal of medicinal chemistry 47**:** 2176-2179.

Sung K, Lee A-R, (1992) Synthesis of [(4,5-disubstituted-4*H* -1,2,4-triazol-3-yl)thio]alkanoic acids and their analogues as possible antiinflammatory agents *J. Het. Chem* ., *29* , 1101-1109.

Tort AB, *et al.* (2007). On the formation of gamma-coherent cell assemblies by oriens lacunosum-moleculare interneurons in the hippocampus. Proceedings of the National Academy of Sciences of the United States of America 104**:** 13490-13495.

Whiting PJ (2003). The GABAA receptor gene family: new opportunities for drug development. Curr Opin Drug Discov Devel 6**:** 648-657.

Yee BK, *et al.* (2004). GABA receptors containing the alpha5 subunit mediate the trace effect in aversive and appetitive conditioning and extinction of conditioned fear. Eur J Neurosci 20**:**1928-1936.

Zhang W, *et al.* (2016). Hyperactive somatostatin interneurons contribute to excitotoxicity in neurodegenerative disorders. Nat Neurosci 19**:** 557-559.

Author contribution:

Alexandra L. Petrache – Performed immunofluorescence studies on mouse brains to characterise the expression of α5 $GABA_A$Rs in different subtypes of interneurons, and assisted in preparing the manuscript.

Archie A. Khan- Designed and produced the new alpha 5 cell line and assisted in preparing the manuscript.

Alessandra Monaco – Synthesised and refined various analogues of alpha 5 NAMs with varying biological activity.

Martin W. Nicholson – Designed and produced the α5β2γ2-$GABA_A$R stable cell line.

Martyna Kuta-Siejkowska - performed molecular docking and identification of the final conformation of the developed NAM.

Shozeb Haider - Computational modelling and assisted in preparing the manuscript.

Stephen Hilton – Developed, refined and synthesised the α5 compounds.

Jasmina N. Jovanovic – Supervised production and characterisation of all HEK293 cell lines stably expressing $GABA_A$Rs which were used in this study.

Afia .B Ali – Designed and coordinated the project, performed and analysed all electrophysiology and neuroanatomy experiments, and prepared the manuscript.

Acknowledgments

Experiments were performed using equipment funded by the Wellcome Trust (UK) and by the Medical Research Council (UK) New Investigators award (AB Ali: GO501263) and MRC PhD studentship (MR/N013867/1).

We would like to thank Dr Andrew Constanti (UCL School of Pharmacy) for his invaluable comments in preparation of this manuscript. We also thank Miss Audrey Crystalia for assisting in the development and characterisation of the α2β2γ2-HEK293 stable cell lines, Professor F. A. Stephenson (UCL School of Pharmacy) for the $GABA_A$R α1 subunit-specific antibody and Professor Jean-Marc Fritschy (University of Zurich) for the $GABA_A$R α5 and γ2 subunit-specific antibodies used for the HEK cell lines.

PV-expressing cells

	Cell density in hippocampal subfields /mm^3			Normalised cell density in hippocampal layers / mm^3				Length of dendrites (μm)		Area of soma (μm^2)
	CA1	CA3	DG	SO	SP	SR	SLM	Primary	Secondary	
Control (n = 20)	569 ± 37	539 ± 120	644 ± 104	589 ± 139	2355 ± 225	216 ± 34	169 ± 16	216 ± 10	125 ± 10	305 ± 13
Epileptic (n = 20)	172 ± 18	170 ± 15	269 ± 44	128 ± 38	847 ± 116	49 ± 8	73 ± 18	163 ± 10	86 ± 8	253 ± 16
CBD_time0 (n = 20)	368 ± 41	329 ± 36	702 ± 53	511 ± 99	1899 ± 257	101 ± 20	89 ± 17	264 ± 9	157 ± 7	290 ± 12
CBD_time90 (n = 20)	357 ± 43	318 ± 15	618 ± 39	543 ± 119	2036 ± 246	111 ± 11	36 ± 16	259 ± 10	151 ± 5	236 ± 8
Control-Epileptic	****	**	**	*	***	****	**	**	**	*
Control-CBD_time0	**					**	*	**	*	
Control-CBD_time90	**					**	***	*		**
Epileptic-CBD_time0	**		***		*			****	****	
Epileptic-CBD_time90	**		**	*	**			****	****	
CBD_time0-CBD_time90										*

CCK-expressing cells

	Cell density in hippocampal subfields /mm^3			Normalised cell density in hippocampal layers / mm^3				Length of dendrites (μm)		Area of soma (μm^2)
	CA1	CA3	DG	SO	SP	SR	SLM	Primary	Secondary	
Control (n = 20)	305 ± 42	272 ± 46	484 ± 121	171 ± 34	563 ± 132	316 ± 62	308 ± 109	164 ± 15	104 ± 14	222 ± 12
Epileptic (n = 20)	89 ± 14	107 ± 7	140 ± 8	40 ± 8	130 ± 30	147 ± 34	42 ± 10	105 ± 7	58 ± 5	193 ± 10
CBD_time0 (n = 20)	283 ± 21	344 ± 38	375 ± 40	231 ± 55	585 ± 85	143 ± 14	317 ± 40	211 ± 7	120 ± 4	201 ± 6
CBD_time90 (n = 20)	307 ± 32	311 ± 33	323 ± 38	239 ± 56	565 ± 96	147 ± 20	394 ± 84	203 ± 7	113 ± 6	213 ± 6
Control-Epileptic	***	**	**			*		***	***	***
Control-CBD_time0						*		**		
Control-CBD_time90						*		*		
Epileptic-CBD_time0	***	***	*	*	**		*	****	****	
Epileptic-CBD_time90	***	**		*	*		**	****	****	**
CBD_time0-CBD_time90										

Results are expressed as mean ± SEM. * *P* ≤ *0.05*, ** *P* ≤ *0.01*, *** *P* ≤ *0.001*, **** *P* ≤ *0.0001*.

A one-way ANOVA with post-hoc Tukey test was used for statistical analyses. Statistical significance was tested between control, epileptic and CBD-treated groups.

Conflict of Interest Statement: None

Figures and Figure Legends

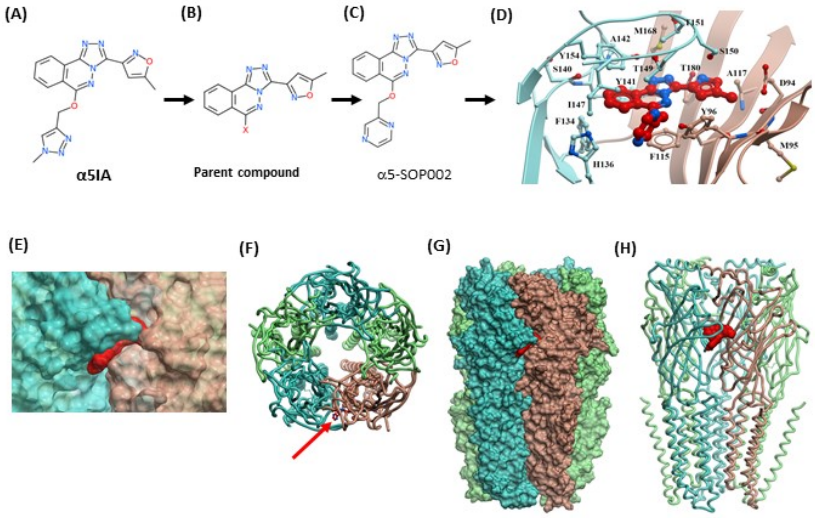

Figure 1

Figure 1**.** **(A-C**) Optimisation of α5IA to α5-SOP002. **(D)**Detailed interactions of α5-SOP002 at the $GABA_AR$ binding site located at the interface between subunit α5 (blue) and γ2 (brown).**(E)** Surface representation of SH-AI-SOP002 (red) interacting with the α5 $GABA_AR$ at the α5 (blue) and γ2 (brown) subunits' interface. **(F)** Upper view of the α5 $GABA_A$ subtype represented by ribbons. The red arrow points at α5-SOP002. Subunits α5 are shown in blue, β3 in green and γ2 in brown. **(G)** Surface and **(H)** ribbon representation of the α5 $GABA_AR$.

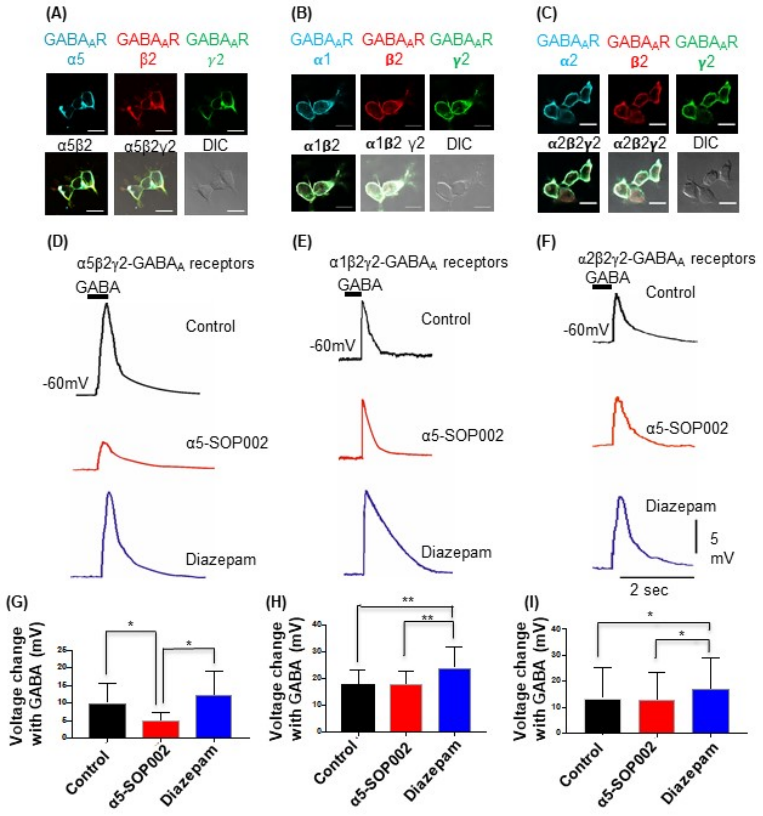

Figure 2

Figure 2. **α5-ΣΟΠ002 σελεστιελψ ταργετς α5 συβυνιτς οφ ΓΑΒΑ$_A$Ρς.** Whole-cell current clamp recordings in α5β2γ2-, α1β2γ2-, and α2β2γ2-HEK293 cells. HEK293 cells stably expressing α5β2γ2- **(A),** α1β2γ2- **(B),** or α2β2γ2-GABA$_A$Rs **(C).** Immunofluorescent imaging with 40x oil immersion objective lens shows cell surface expression of α5, α1 or α2- (cyan), β2- (red), and γ2-GABA$_A$R subunits (green). (A-C) also show all the three channels merged showing α-, β2-, and γ2-GABA$_A$R subunit co-localisation at the cell surface (white) along with the DIC image of the cells. Scale bar represents 10 μm. All three stable cell lines responded to 10 μM puff-applied GABA **(D-F)** in control extracellular solution (black traces), extracellular solution containing 1 μM α5-SOP002 (red traces), and following puff-application of 1 μM diazepam (blue traces) at a holding membrane potential of -60 mV. The corresponding plots for α5β2γ2-HEK293 cells **(G-I)** show the changes in membrane potential in response to 10 μM GABA puffed locally, in the presence of

bath-applied α5-SOP002, and in the presence of diazepam. Only the α5β2γ2-HEK293 cells showed an inverse agonist effect (response to GABA) of α5-SOP002. All three cell lines however, showed an enhancement of response to GABA in the presence of diazepam. Statistically significant data are shown with * for P <0.05 and ** for P<0.01.

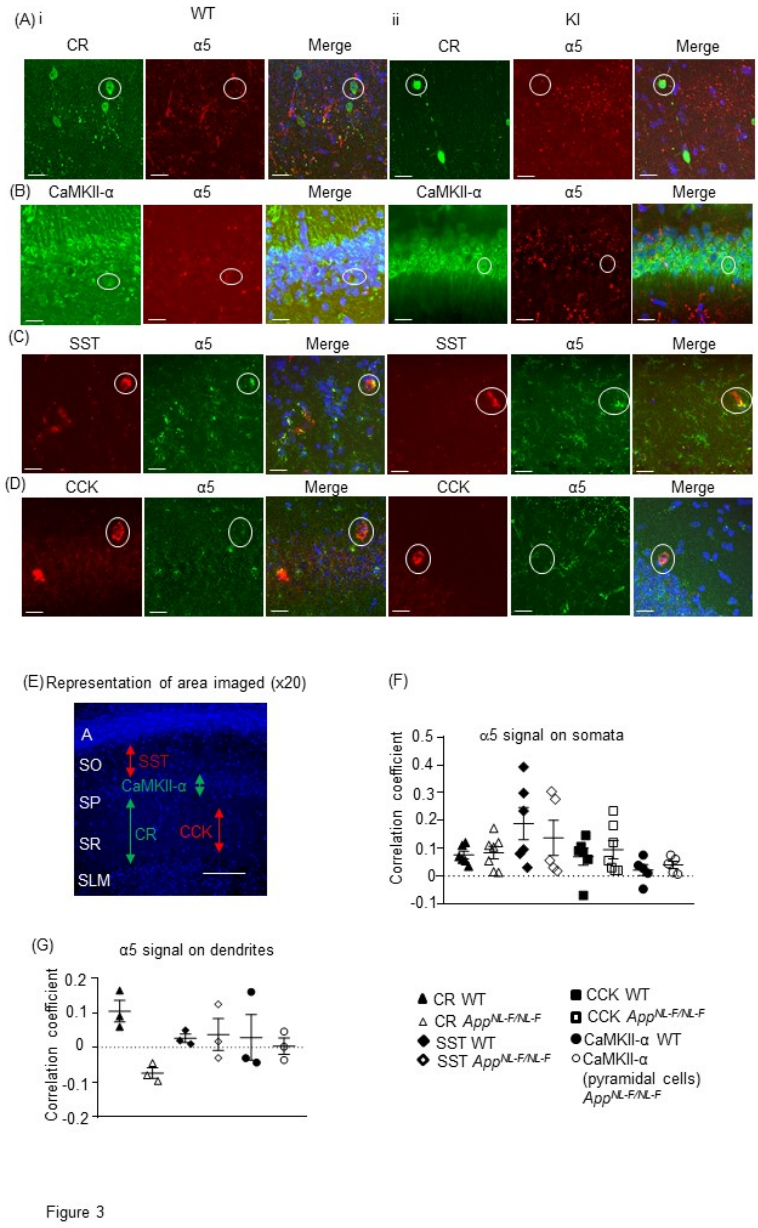

Figure 3

Figure 3. **Εξπρεσσιον οφ α5 συβυνιτ-ςοντ αινινγ ΓΑΒΑ$_A$Ρς ιν ῞Α1 . (A-D)** Confocal microscopy Z-stacks at 63× magnification showing α5 subunit-containing GABA$_A$R expression on pyramidal neurons (CaMKII- α, green, FITC), CR interneurons (green, Alexa 488), SST interneurons (red, Texas Red), and CCK interneurons (red, Texas Red) in wild-type**(i)** and $App^{NL-F/NL-F}$ animals**(ii)** . Panels show individual channels and merged image with the nuclear stain DAPI (blue). Representative cells are outlined with white circles. **(E)** Representative image taken at 20× magnification to exemplify the region of data acquisition.

Layers are labelled: alveus (A), stratum oriens (SO), stratum pyramidale (SP), stratum radiatum (SR), stratum lacunosum moleculare (SLM). The image is labelled with the cell names in the locations they were imaged. **(F)** Analysis of α5 subunit-containing $GABA_AR$ expression on the soma of the four types of cells investigated. **(G)** Analysis of α5 subunit-containing $GABA_AR$ signal on the dendrites of CR cells, SST cells and pyramidal neurons **(F-G)** Results are expressed as a scatter plot ± standard error of the mean (results not significant, $P > 0.05$), of Pearson correlation coefficient as a measure of colocalisation, after application of Fisher's transformation.

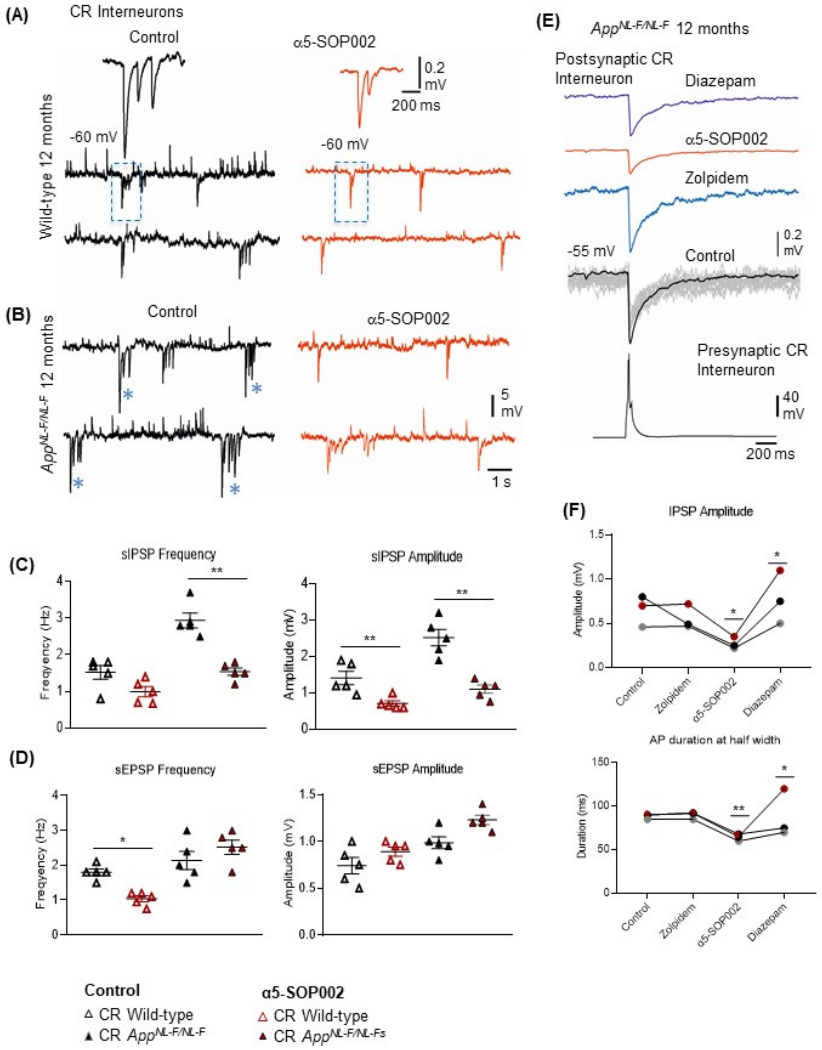

Figure 4

Figure 4. **Ἀlρετινιν (ˆP)-εξπρεσσινγ ιντερνευρονς αρε φυνςτιοναλλψ ρεστορεδ βψ NAM οφ α5 συβυνιτ-ςοντανινγ ΓΑΒΑ$_A$Ρς ιν $Aππ^{NΛ\text{-}Φ/NΛ\text{-}Φ}$μιςε. A, B)** Whole-cell current-clamp recordings of spontaneous inhibitory/excitatory postsynaptic potentials (sIPSPs and sEPSPs) recorded in

CR cells in CA1 of 12 month old wild-type and$App^{NL\text{-}F/NL\text{-}F}$ mice, at membrane potentials of -60 mV in control conditions, and after bath-application of α5-SOP002 (red traces). The squares indicate where synaptic events have been enlarged and shown in the inserts. *Indicate, an usually high sIPSPs recorded in the AD model. **C, D)** Bar graphs show the average sIPSP and sEPSP amplitude and frequency at -60 mV in CR cells recorded in wild-type mice and the $App^{NL\text{-}F/NL\text{-}F}$ mouse model. These data suggest a significantly enhanced amplitude and frequency of inhibition in the AD model, which was "normalised" to control values after bath- application of α5-SOP002. **E)** Paired recording obtained between two putative CR cells recorded in SR of CA1 in the AD model. The unitary IPSPs were not sensitive to zolpidem, reduced by α5-SOP002, and then enhanced by subsequent addition of diazepam, indicating α5 pharmacology. **F)** Line graphs show the average unitary IPSP amplitude and width at half amplitude change for each paired recording between 2 CR cells, in control, and after bath-application of zolpidem, α5-SOP002 and diazepam, recorded at -55 mV in $App^{NL\text{-}F/NL\text{-}F}$ mouse model. * $P<0.05$, ** $P< 0.01$, *** $P < 0.001$, **** $P < 0.0001$.

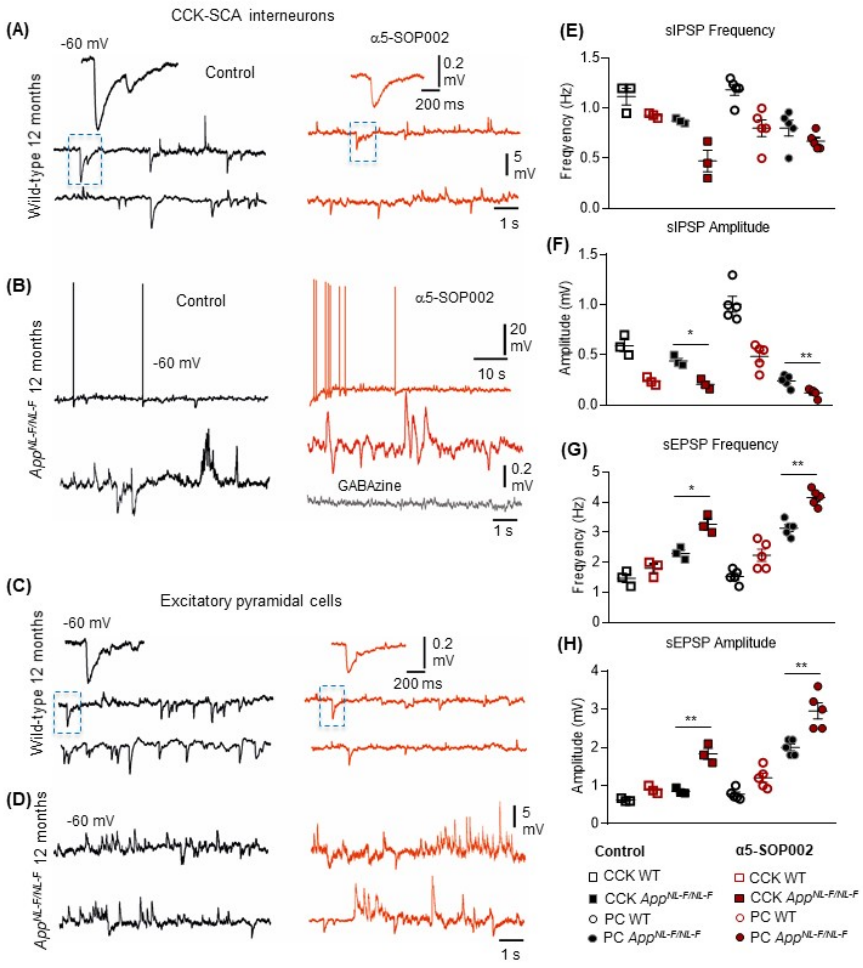

Figure 5

Figure 5. **""K ιντερνευρονς ανδ πψραμιδαλ χελλς αρε φυρτηερ χομπρομισεδ βψ NAM οφ α5 συβυνιτ-χονταινινγ ΓΑΒΑ$_A$Pς ιν$A\pi\pi^{NA\text{-}\Phi/NA\text{-}\Phi}$ mice. A-B and C-D)** Whole-cell current-clamp recordings illustrating sIPSPs and sEPSPs recorded in CCK-SCA cells (A-B) and pyramidal cells (C-D) in CA1 of 12 month old wild-type and $App^{NL\text{-}F/NL\text{-}F}$ mice, recorded at a membrane potential of -60 mV in control conditions and after bath-application of α5-SOP002. Bath-application of the α5-SOP002 resulted in a reduction in sIPSP amplitude and frequency, but also increased membrane excitation in both cell types, thus further increasing the aberrant hyperexcitability in the AD model. **E-F and G-H)** Bar graphs show the overall pharmacological change after applying α5-SOP002 in CCK-SCA and pyramidal cells recorded from wild-type and $App^{NL\text{-}F/NL\text{-}F}$ mice at 10-12 months. * P <0.05, ** P < 0.01, *** P< 0.001, **** P < 0.0001 (see Table 1 for details).

Cell subtype	**CR cells n=5**	**CR cells n=5**	**CCK cells n=3**	**CC**
sIPSP Frequency (Hz)	**Control**	**α5-ΣΟΠ002**	**Control**	**α5**
Wild-type	1.52 ± 0.19	0.99 ± 0.14	1.12 ± 0.08	0.9
$App^{NL\text{-}F/NL\text{-}F}$	2.94 ± 0.20	1.54 ± 0.10**	0.87 ± 0.01	0.4
sIPSP Amplitude (Hz)	**sIPSP Amplitude (Hz)**	**sIPSP Amplitude (Hz)**	**sIPSP Amplitude (Hz)**	**sIP**
Wild-type	1.41 ± 0.19	0.71 ± 0.07**	0.59 ± 0.06	0.2
$App^{NL\text{-}F/NL\text{-}F}$	2.52 ± 0.23	1.10 ± 0.11**	0.44 ± 0.03	0.2
sEPSP Frequency (mV)	**sEPSP Frequency (mV)**	**sEPSP Frequency (mV)**	**sEPSP Frequency (mV)**	**sE**
Wild-type	1.8 ± 0.09	1.4 ± 0.09 *	1.47 ± 0.15	1.8
$App^{NL\text{-}F/NL\text{-}F}$	2.14 ± 0.26	2.52 ± 0.20	2.3 ± 0.12	3.2
sEPSP Amplitude (Hz)	**sEPSP Amplitude (Hz)**	**sEPSP Amplitude (Hz)**	**sEPSP Amplitude (Hz)**	**sE**
Wild-type	0.74 ± 0.09	0.89 ± 0.05	0.62 ± 0.02	0.8
$App^{NL\text{-}F/NL\text{-}F}$	0.99 ± 0.06	1.23 ± 0.05	0.86 ± 0.05	1.8

Table 1. **Changes of spontaneous synaptic events recorded in CR, CCK-SCA and pyramidal cells after bath-application of a5-SOP002 in 10-12 months of age-matched, wild-type and $APP^{NL\text{-}F/NL\text{-}F}$ mice.** sIPSP, spontaneous inhibitory postsynaptic potential. sEPSP, spontaneous excitatory postsynaptic potentials; * $P < 0.05$, ** P <0.01 . Values represent average values in control and after bath-application of a5-SOP002 ± SEM. A one-way ANOVA followed by post-hoc Tukey's test for multiple comparisons was used to determine the statistical value. A paired, two-tailed Student's t-test was utilised for direct comparison between two cohorts when Tukey's test was not utilised. Sample size n denotes the number of animals (one cell per animal was recorded in these experiments).